

43. We thank J. Valcarcel and I. Mattaj for suggestions and critical reading of the manuscript; the European Large Scale facility in Frankfurt, Germany, and W. Bernel (Bruker, Karlsruhe, Germany) for time on the 800-MHz spectrometer; and M. Nilges and J. Linge for ARIA software. Support from EMBL and

the Deutsche Forschungsgemeinschaft (M.S.); Fonds voor Wetenschappelijk Onderzoek (FWO), Vlaanderen, Netherlands, and European Molecular Biology Organization (I.L.); Fundação para a Ciência e Tecnologia (A.C.M.); and the Swiss National Science Foundation (SNF) and the Canton of Geneva

(A.K.) is acknowledged. Coordinates for the NMR structure of the SF1/RNA complex have been deposited in the Protein Data Bank under accession code 1K1G.

25 July 2001; accepted 13 September 2001

Mammalian TOR: A Homeostatic ATP Sensor

Patrick B. Dennis,¹ Anja Jaeschke,¹ Masao Saitoh,¹ Brian Fowler,² Sara C. Kozma,¹ George Thomas^{1*}

The bacterial macrolide rapamycin is an efficacious anticancer agent against solid tumors. In a hypoxic environment, the increase in mass of solid tumors is dependent on the recruitment of mitogens and nutrients. When nutrient concentrations change, particularly those of essential amino acids, the mammalian Target of Rapamycin (mTOR) functions in regulatory pathways that control ribosome biogenesis and cell growth. In bacteria, ribosome biogenesis is independently regulated by amino acids and adenosine triphosphate (ATP). Here we demonstrate that the mTOR pathway is influenced by the intracellular concentration of ATP, independent of the abundance of amino acids, and that mTOR itself is an ATP sensor.

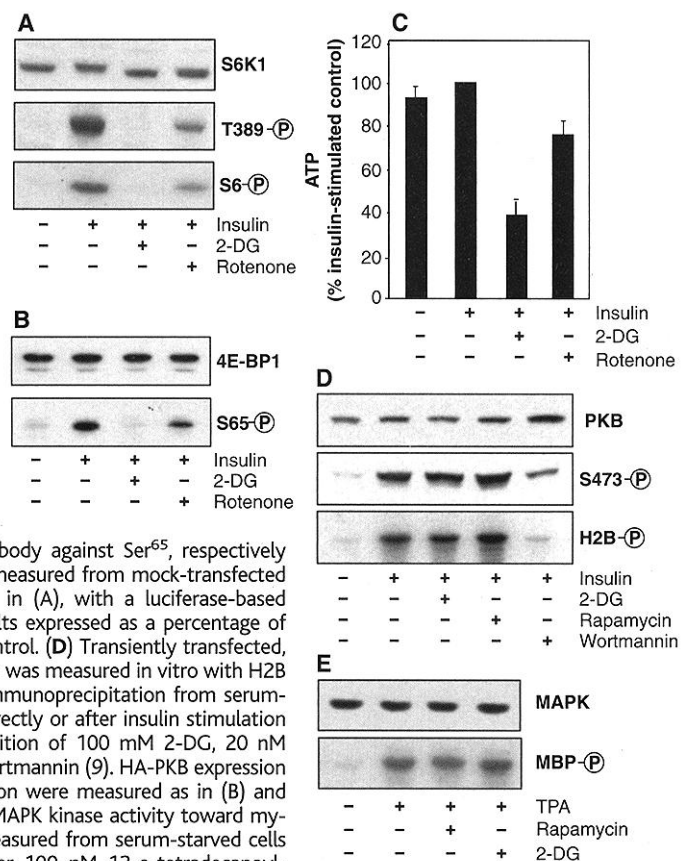
The survival of organisms is dependent on their ability to maintain cellular homeostasis. Environmental cues are deciphered by cellular regulatory elements, which adjust an organism's metabolic state to reflect external conditions. The phosphatidylinositol kinase-related family of protein kinases contains a number of critical effectors that sense environmental factors that control the ability of an organism to survive. One member of the family is mTOR, which resides at the interface between nutrient sensing and the regulation of major metabolic responses (1–3). Depending on mitogen and amino acid availability, mTOR positively regulates translation and ribosome biogenesis while negatively controlling autophagy (1), suggesting that mTOR sets protein synthetic rates as a function of the availability of translational precursors (4, 5). In response to mitogens and amino acids, mTOR phosphorylates and controls the activities of two key translational regulators, S6 kinase 1 (S6K1) and initiation factor 4E binding protein (4E-BP1) (2). However, changes in mTOR activity in vitro, after either mitogen or amino acid treatment, have been small and controversial (2, 3). The importance of understanding the molecular mechanisms that control mTOR function is underscored by recent phase I clinical trials showing that rapamycin is efficacious in the treatment of solid tumors in patients with metastatic renal

cell carcinoma and non-small cell lung, prostate, and breast cancer (6).

Protein synthesis is the major energy-consuming process in the cell (7). In bacteria,

protein synthesis and cell growth are linked by ribosome biogenesis, which is independently controlled by amino acid and adenosine triphosphate (ATP) availability (8). Because mTOR is sensitive to amino acids and regulates ribosome biogenesis (1–3), we tested its activity for sensitivity to alterations in intracellular ATP concentrations. We used insulin-induced S6K1 activation and 4E-BP1 phosphorylation as reporters for mTOR function in the presence of glycolytic or mitochondrial inhibitors (9). The glycolytic inhibitor 2-deoxyglucose (2-DG) was more effective in inhibiting S6K1 Thr³⁸⁹ phosphorylation and S6K1 activation than was the mitochondrial inhibitor rotenone (Fig. 1A). Similar results were obtained when an mTOR-mediated phosphorylation site in 4E-BP1 (Ser⁶⁵) was measured (Fig. 1B) and when iodoacetic acid and dinitrophenol were used as glycolytic and mitochondrial inhibitors, respectively (10). The effectiveness of each agent in inhibiting S6K1 activation par-

Fig. 1. The effects of metabolic inhibitors. (A) Serum-starved HEK293 cells were extracted directly or stimulated with 200 nM insulin in the presence of 100 mM 2-DG or 20 μM rotenone for 30 min. S6K1 levels and Thr³⁸⁹ phosphorylation were measured by Western blot analysis (9). S6K1 activity was assayed as described previously (22). (B) The expression and phosphorylation of transiently transfected HA-4E-BP1 was measured as in (A), with a polyclonal antibody to HA and phosphospecific antibody against Ser⁶⁵, respectively (9). (C) ATP levels were measured from mock-transfected HEK293 cells treated as in (A), with a luciferase-based assay (11), with the results expressed as a percentage of the insulin-stimulated control. (D) Transiently transfected, HA-tagged PKB activation was measured in vitro with H2B as substrate (22) after immunoprecipitation from serum-starved cells extracted directly or after insulin stimulation with or without the addition of 100 mM 2-DG, 20 nM rapamycin, or 100 nM wortmannin (9). HA-PKB expression and Ser⁴⁷³ phosphorylation were measured as in (B) and (9), respectively. (E) HA-MAPK kinase activity toward myelin basic protein was measured from serum-starved cells extracted directly or after 100 nM 12-*o*-tetradecanoylphorbol-13-acetate (TPA) stimulation in the presence or absence of 20 nM rapamycin or 100 mM 2-DG for 30 min (22). All results and the SE in (C) are representative of at least three independent experiments.



¹The Friedrich Miescher Institute for Biomedical Research, Maulbeerstrasse 66, CH-4058, Basel, Switzerland. ²University Childrens Hospital CH-4005, Basel, Switzerland.

*To whom correspondence should be addressed. E-mail: gthomas@fmi.ch

alleled its ability to lower ATP concentrations, as measured in a luciferase reporter assay (Fig. 1C) (11). The glycolytic inhibitors may be more effective in reducing ATP concentrations in transformed HEK293 cells because those cells predominately use anaerobic respiration to produce ATP (12, 13). The modest effect of rotenone in reducing ATP concentrations, as compared with its effects on S6K1 and 4E-BP1 phosphorylation, suggested that the inhibitors were not generally toxic. To verify this, we tested the effect of 2-DG on protein kinase B (PKB) and mitogen-activated protein kinase (MAPK). Like rapamycin, 2-DG did not inhibit insulin-induced activation of PKB, which was sensitive to the phosphatidylinositolide-3-OH kinase (PI3K) inhibitor wortmannin, as judged by Ser⁴⁷³ phosphorylation and in vitro phosphorylation of histone 2B (H2B) (Fig. 1D). Also, 2-DG had no effect on TPA-induced MAPK activation, with myelin basic protein (MBP) as substrate (Fig. 1E). Hence, the 2-DG-induced reduction in ATP concentrations appears to selectively influence signaling to S6K1 and 4E-BP1.

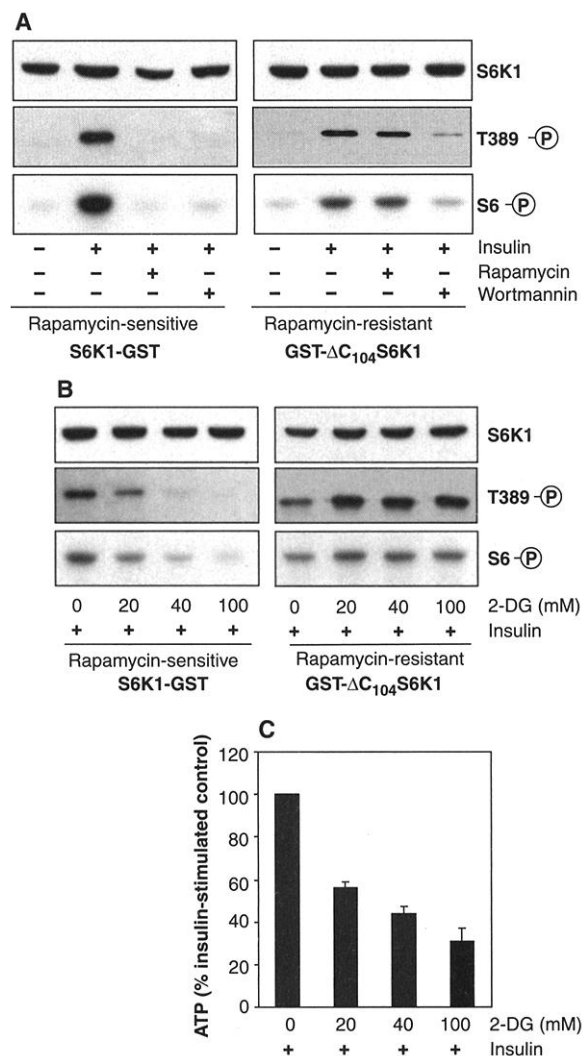
To assess whether the inhibitory effects of 2-DG on S6K1 activation were mediated by mTOR, we used a rapamycin-resistant allele of S6K1. Rapamycin resistance was conferred by fusing glutathione S-transferase (GST) to the NH₂-terminus of S6K1 and truncating the COOH-terminus, creating a construct termed GST-ΔC-S6K1 (14). Both S6K1, having a COOH-terminal GST tag (S6K1-GST), and GST-ΔC-S6K1 were phosphorylated and activated by insulin in a wortmannin-sensitive manner. However, only GST-ΔC-S6K1 was resistant to inhibition by rapamycin (Fig. 2A). 2-DG reduced insulin-induced activation of S6K1-GST (Fig. 2B) in a dose-dependent manner, paralleling its effect on intracellular ATP concentrations (Fig. 2C). In contrast, insulin-induced activation of GST-ΔC-S6K1 was unaffected by 2-DG treatment (Fig. 2B). Thus, 2-DG appears to selectively inhibit signaling to mTOR effectors, supporting a model whereby mTOR is controlled by intracellular ATP concentrations.

Because mTOR signaling is dependent on concentrations of aminoacylated tRNAs (5), the effects of ATP on S6K1 and 4E-BP1 may be indirect, occurring through inhibition of

tRNA aminoacylation. To examine this possibility, we analyzed total cellular tRNA on acid-urea polyacrylamide gels, which resolve aminoacylated from nonacylated tRNA (15). Neither insulin stimulation nor 2-DG treatment had an effect on total amounts of aminoacylated tRNA (Fig. 3A). Unexpectedly, amino acid deprivation also had no effect (Fig. 3A), even though such treatment was sufficient to completely block phosphorylation of S6K1 and 4E-BP1 (Fig. 3B). To further test this finding, we examined selected tRNAs by Northern blot analysis. As with total tRNA, none of the three treatments had an effect on the aminoacylation status of leucyl, histidyl, or threonyl tRNA (Fig. 3A) (10), indicating that amino acid pools, rather than amounts of aminoacylated tRNA, were important for mTOR signaling (16). Indeed, amino acid deprivation resulted in a decrease in the amounts of essential amino acids, particularly the branched-chain amino acids, whereas 2-DG had little effect (Fig. 3C) (10). Furthermore, amino acid deprivation had no effect on concentrations of ATP (Fig. 3D). Thus, regulation of mTOR by ATP is independent of amino acids pools.

Reducing ATP concentrations could lead to a stable change in mTOR activity, through a posttranslational modification, or ATP could directly affect mTOR activity. To test the first possibility, we transiently expressed hemagglutinin (HA) epitope-tagged mTOR in HEK293 and measured its activity after treatment of cells with 2-DG (17). Although such treatment blocked insulin-induced activation of S6K1 (Fig. 1A), it had no effect on the kinase activity of mTOR in vitro toward Thr³⁸⁹ of S6K1 (Fig. 4A). Indeed, neither amino acid deprivation, insulin stimulation, nor transient expression of an activated allele of PI3K affected mTOR kinase activity in vitro (Fig. 4, A and B), despite their ability in the intact cell to affect Thr³⁸⁹ phosphorylation and S6K1 activation (Figs. 3B and 4C). Next, we measured mTOR activity in vitro at ATP concentrations that approached physiological levels of 1 to 5 mM in mammalian cells (18). Specific activity of mTOR increased up to ~1 mM ATP, saturating at around 2 or 3 mM ATP, whereas the catalytically inactive mTOR mutant did not phosphorylate Thr³⁸⁹ (Fig. 4D). On the basis of these values, we calculated a K_m (Michaelis constant) for ATP of slightly greater than 1 mM (17). Most protein kinases analyzed to date show an apparent K_m for ATP of 10 to 20 μM (19), one-hundredth to one-fiftieth of that observed for mTOR. Because mTOR also phosphorylates several sites in 4E-BP1, including Ser⁶⁵ (2), we also assayed the ATP requirement of mTOR for Ser⁶⁵ of 4E-BP1. Using the same assay conditions described for Thr³⁸⁹ phosphorylation in S6K1, we obtained almost identical results for Ser⁶⁵ phos-

Fig. 2. Specific inhibition of mTOR-signaling by 2-DG. (A) S6K1-GST and GST-ΔC-S6K1 from transiently transfected, serum-starved HEK293 cells were extracted directly or after insulin stimulation with or without the addition of 20 nM rapamycin or 100 nM wortmannin (9). Kinase activities, expression levels, and T389 phosphorylation were as in Fig. 1A and (22). (B), Expression and activity of S6K1-GST or GST-ΔC-S6K1 were measured after insulin stimulation alone or with increasing amounts of 2-DG as in (A). (C) Mock-transfected HEK293 cells were treated as in (B) and extracted for ATP analysis as in Fig. 1C. Results and SE in (C) are typical of at least two independent experiments.



REPORTS

phorylation (Fig. 4D). These findings sustain the role of mTOR as an ATP effector and suggest that it is a direct sensor of ATP in the cell.

Our data support the hypothesis that intracellular concentrations of ATP directly regulate mTOR, whereas mTOR regulation by amino acids uses a separate mechanism (Fig. 4E). Likewise, in bacteria, amino acids and ATP are

sensed by different mechanisms. Amino acid deprivation in bacteria triggers the "stringent response," the production of the guanosine triphosphate derivative ppGpp, which blocks ribosome biogenesis by directly binding to rRNA polymerase (δ). In contrast, as ATP concentrations begin to decrease in growing bacteria, the rate of initiation at rRNA promoters decreases because of the rapid decay of open

promoter complexes (20). Here we propose that, as ATP is used in eukaryotic cells, mTOR functions as a homeostatic sensor, adjusting the rate of ribosome biogenesis to reflect intracellular ATP concentrations (Fig. 4E). Increased ribosome biogenesis is a predictive indicator of solid tumor progression (21), and in such tumors, metabolic flux is redirected to glycolysis, leading to the more rapid production of ATP (12, 13). If tumors gain an mTOR-specific growth advantage because of increased production of ATP, they may be more susceptible to the effects of rapamycin.

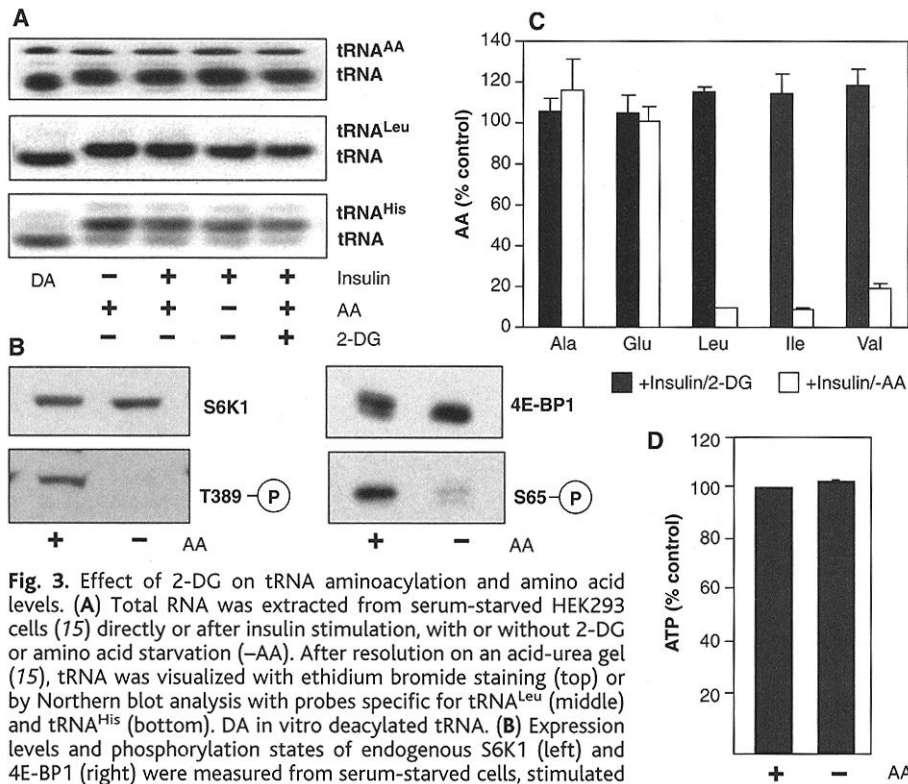
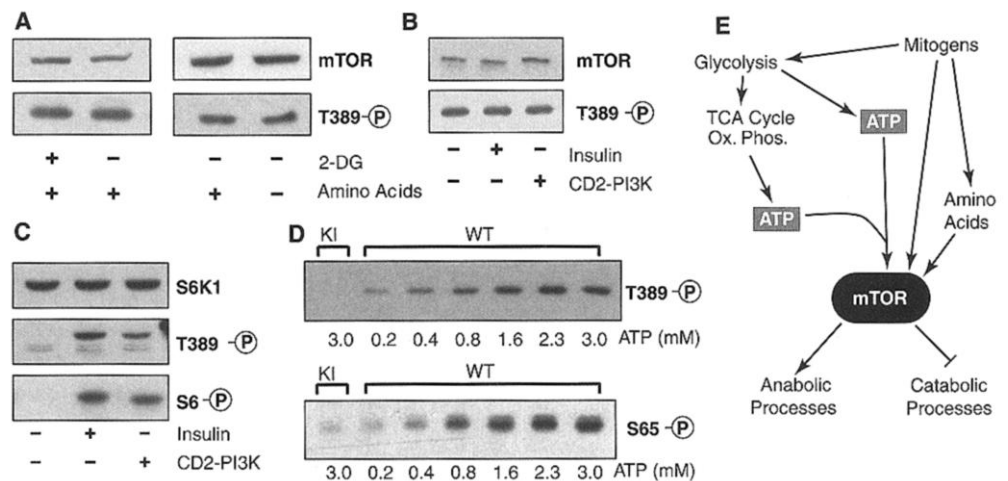


Fig. 3. Effect of 2-DG on tRNA aminoacylation and amino acid levels. (A) Total RNA was extracted from serum-starved HEK293 cells (15) directly or after insulin stimulation, with or without 2-DG or amino acid starvation (-AA). After resolution on an acid-urea gel (15), tRNA was visualized with ethidium bromide staining (top) or by Northern blot analysis with probes specific for tRNA^{Leu} (middle) and tRNA^{His} (bottom). DA in vitro deacylated tRNA. (B) Expression levels and phosphorylation states of endogenous S6K1 (left) and 4E-BP1 (right) were measured from serum-starved cells, stimulated with insulin in the presence or absence of amino acids in the media as in Fig. 1A and (9). (C) Levels of individual amino acids were measured in extracts prepared from insulin-stimulated HEK293 cells in the presence or absence of amino acids or with 100 mM 2-DG treatment (24) and expressed as a percentage of the insulin-stimulated control in the presence of amino acids. (D) Cells treated as in (B) were extracted for ATP analysis (17), and the results were expressed as a percentage of the insulin-stimulated control in the presence of amino acids. Results and SE derived in (C) and (D) are typical of at least two independent experiments.

Fig. 4. mTOR activity requires high ATP concentrations. (A) HA-tagged, wild-type mTOR (HA-mTORwt) was obtained from serum-starved HEK293 cells that were insulin-stimulated with or without 100 mM 2-DG treatment (left) or amino acid starvation (right). HA-mTORwt was assayed for Thr³⁸⁹ kinase activity, with a kinase inactive mutant of S6K1 (D3E,K100Q-GST) as substrate (17). (B) HA-mTORwt was transiently expressed alone or with a constitutively membrane-targeted PI3K (CD2-PI3K) and then extracted directly or stimulated with insulin before extraction. HA-mTOR kinase was measured as in (A). (C) Myc-tagged, wild-type S6K1 was expressed alone or with CD2-PI3K in starved or insulin-stimulated HEK293 cells. S6K1 kinase activity was assayed as in Fig. 1A after immunoprecipitation with an antibody to myc. (D) The expressions and activities of HA-mTORwt (WT) and kinase inactive (KI) were assayed against S6K1 Thr³⁸⁹ (top) or 4E-BP1 Ser⁶⁵ (bottom) (9). ATP concentrations used in the assay are indicated below each panel. (E) The schematic demonstrates distinct control of mTOR activity by ATP and amino acids.



References and Notes

- P. B. Dennis, S. Fumagalli, G. Thomas, *Curr. Opin. Genet. Dev.* **9**, 49 (1999).
- A. C. Gingras, B. Raught, N. Sonenberg, *Genes Dev.* **15**, 807 (2001).
- T. Schmelzle, M. N. Hall, *Cell* **103**, 193 (2000).
- K. Hara et al., *J. Biol. Chem.* **273**, 14484 (1998).
- Y. Iiboshi et al., *J. Biol. Chem.* **274**, 1092 (1999).
- M. Hidalgo, E. K. Rowinsky, *Oncogene* **19**, 6680 (2000).
- E. V. Schmidt, *Oncogene* **18**, 2988 (1999).
- J. Roberts, *Science* **278**, 2073 (1997).
- HEK293 cells were seeded and maintained as previously described (22). Confluent cells were serum starved for 20 hours and then treated simultaneously with 200 nM insulin and the indicated amounts of 2-deoxyglucose and rotenone for 30 min. Cell extraction, kinase assays, and Western blots were performed as described (22). Phosphospecific antibodies and the antibody to HA were obtained from New England Biolabs and Santa Cruz Biotechnology, respectively. Rapamycin and wortmannin were added to serum-starved cells 30 min before insulin stimulation.
- P. B. Dennis, A. Jaeschke, M. Saito, S. C. Kozma, G. Thomas, unpublished data.
- HEK293 cells were treated as previously described (22). To generate extracts for ATP assays, we washed cells twice with 10 ml of ice-cold phosphate-buffered saline (PBS), drained them thoroughly, scraped them into 1 ml of buffer [100 mM tris-HCl and 4 mM EDTA (pH 7.75)], and transferred them into an Eppendorf tube before flash freezing in liquid nitrogen. The frozen cells were boiled for 3 min, placed on ice for 5 min, and then centrifuged at 13,000 rpm for 5 min at 4°C. ATP levels in the extract were measured in a microtiter plate by a luciferase-based assay (Roche, ATP Bioluminescence Assay Kit CLS II) with a Microumat LB96P microtiter plate reader (EG&G Berthold).

12. T. Pfeiffer, S. Schuster, S. Bonhoeffer, *Science* **292**, 504 (2001).
13. C. V. Dang, G. L. Semenza, *Trends Biochem. Sci.* **24**, 68 (1999).
14. Construction and assay of the S6K1-GST construct were described previously (22). For the construction of the GST- Δ C-S6K1 and D3E,K100Q-S6K1-GST plasmids, similar cloning strategies were used.
15. Total RNA was isolated from HEK293 cells as described (23). Deacylation of tRNA was accomplished by mild alkaline hydrolysis in 0.1 M tris-HCl (pH 8.0) at 75°C for 5 min. Total RNA was electrophoresed as described (23), and resolved tRNA was visualized with ethidium bromide staining before being transferred to a nylon membrane by electroblotting. The individual tRNA species were probed with radiolabeled oligonucleotides as follows: for tRNA^{Leu}, 5'-GCGCCTTAGACCCTCGGCCACG-3'; for tRNA^{His}, 5'-GGTCCCGTACTCGGATTCGAACCG-3'; and for tRNA^{Thr}, 5'-GCGAGAATTGAACCTCGCG-3'.
16. C. J. Lynch, H. L. Fox, T. C. Vary, L. S. Jefferson, S. R. Kimball, *J. Cell. Biochem.* **77**, 234 (2000).
17. Transiently transfected, HA-tagged mTOR from HEK293 cells was extracted after a 16-hour serum

- starvation and immunoprecipitated with a monoclonal antibody to HA. The immunocomplex was washed once with 1 M NaCl in assay buffer [30 mM Mops (pH 7.5), 5 mM NaF, 20 mM β -glycerol phosphate, 1 mM dithioerythritol, 0.1 % Triton X-100, and 10 % glycerol] and twice with assay buffer alone. 1 μ g of a kinase-inactive, purified, soluble S6K1 substrate (S6K1-D3E,K100Q-GST) or GST-4E-BP1 was added along with assay buffer containing 10 mM MgCl₂ and 1 mM ATP and incubated for 30 min at 30°C. Quantitation for K_m measurements was carried out with scanning densitometry and ImageQuant software (Molecular Dynamics).
18. F. M. Gribble *et al.*, *J. Biol. Chem.* **275**, 30046 (2000).
19. A. M. Edelman, D. K. Blumenthal, E. G. Krebs, *Annu. Rev. Biochem.* **56**, 567 (1987).
20. T. Gaal, M. S. Bartlett, W. Ross, C. L. Turnbough Jr., R. L. Gourse, *Science* **278**, 2092 (1997).
21. M. Derenzini *et al.*, *J. Pathol.* **191**, 181 (2000).
22. N. Pullen *et al.*, *Science* **279**, 707 (1998).
23. J. A. Enriquez, G. Attardi, *Methods Enzymol.* **264**, 183 (1996).
24. Confluent cultures of HEK293 cells were treated as described (9), washed with PBS, and drained thor-

- oughly. The cells were then scraped into 500 μ l of water and sonicated with four 10-s pulses. Cell debris was removed by centrifugation, and sulfosalicylic acid was added to the supernatant to a final concentration of 2%. The samples were then placed on ice for 30 min followed by centrifugation to remove precipitated proteins. The extracts were then analyzed for amino acid content with a Biochrom 20 plus amino acid analyzer (Amersham-Pharmacia Biotech).
25. We thank W. Filipowicz, W. Krek, and M. Hall for their critical reading of the manuscript. We are also indebted to D. Cantrell for the CD2-PI3K construct, S. Schreiber for the human mTOR cDNA, and N. Pullen for the generation of a number of the S6K1 constructs used. We also thank P. Cohen and T. Hunter for useful advice with regard to the K_m of kinases for ATP. A.J. and M.S. were supported by fellowships from the Deutsche Forschungsgemeinschaft and European Molecular Biology Organization, and the Swiss Cancer League and the Novartis Research Foundation supported this project.

10 August 2001; accepted 10 September 2001

Dynamic Disruptions in Nuclear Envelope Architecture and Integrity Induced by HIV-1 Vpr

Carlos M. C. de Noronha,¹ Michael P. Sherman,^{1,2} Harrison W. Lin,¹ Marielle V. Cavrois,¹ Robert D. Moir,⁴ Robert D. Goldman,⁴ Warner C. Greene^{1,2,3*}

Human immunodeficiency virus-1 (HIV-1) Vpr expression halts the proliferation of human cells at or near the G₂ cell-cycle checkpoint. The transition from G₂ to mitosis is normally controlled by changes in the state of phosphorylation and subcellular compartmentalization of key cell-cycle regulatory proteins. In studies of the intracellular trafficking of these regulators, we unexpectedly found that wild-type Vpr, but not Vpr mutants impaired for G₂ arrest, induced transient, localized herniations in the nuclear envelope (NE). These herniations were associated with defects in the nuclear lamina. Intermittently, these herniations ruptured, resulting in the mixing of nuclear and cytoplasmic components. These Vpr-induced NE changes probably contribute to the observed cell-cycle arrest.

HIV-1 Vpr is a highly conserved, virion-associated (1), nucleocytoplasmic shuttling (2) protein that blocks proliferating CD4⁺ T cells at the G₂ cell-cycle checkpoint (3, 4). This property of Vpr enhances viral replication because HIV-1 transcription is more active during G₂ (5). Vpr also increases HIV-1 replication in nondividing macrophages, possibly by facilitating, with other viral components (6–11), nuclear uptake of the large (56 nm) viral preintegration complex (PIC) (12–14). Although Vpr has been shown to interact with various host proteins (15–19), the mo-

lecular mechanism underlying Vpr-induced cell-cycle arrest remains unknown.

The transition from G₂ to mitosis depends upon activation of the cyclin B1–Cdc2 kinase complex and its entry into the nucleus during prophase (20). The activity of Cdc2 is regulated in an opposing manner by the Cdc25C phosphatase (21, 22) and the Wee1 and Myt-1 kinases (23, 24). The functions of Cdc25C and Wee1 are regulated not only by changes in their overall phosphorylation but also by changes in their subcellular localization. During S phase, Cdc25C predominantly resides in the cytoplasm, reflecting its assembly with a 14-3-3 protein (25), whereas Wee1 is expressed in the nucleus. During prophase, both of these proteins assume a “whole cell” pattern of expression. Our initial aim was to explore whether HIV-1 Vpr alters the nucleocytoplasmic trafficking of Wee1, Cdc25C, and cyclin B1. We used video fluorescence

microscopy to monitor the movement of these proteins labeled by fusion to either green or red fluorescent protein (GFP, RFP) in synchronized HeLa cell cultures cotransfected with Vpr or control expression plasmids. The dynamic changes are more readily apparent in the Web-based videos (26) than in the still pictures presented in the figures. When expressed alone, Wee1-GFP was observed in cell nuclei during the S and G₂ phases (Fig. 1A and Web fig. 1A). Coincident with the entry of cells into mitosis and NE breakdown, Wee1-GFP displayed a whole-cell pattern of epifluorescence (Fig. 1B and Web fig. 1A). During re-formation of the nuclear membrane in telophase, Wee1-GFP rapidly entered the daughter cell nuclei (Fig. 1, C and D, and Web fig. 1A). In the presence of Vpr, the pattern of Wee1-GFP epifluorescence was markedly different (Fig. 1, E to L, and Web fig. 1B). Notably, prominent, transient herniations formed at the apices of the oblong nuclei (Fig. 1, E to H, and Web fig. 1B). Intermittently, these herniations ruptured, releasing Wee1-GFP into the cytoplasm (Fig. 1, I to L, and Web fig. 1B). However, within 3 to 4 hours, Wee1-GFP was reimported into the nucleus (Fig. 1, K and L, and Web fig. 1B). Consistent with the cell cycle-arresting properties of Vpr, little or no mitosis was observed in these Vpr-expressing cells. Conversely, nonarresting Vpr mutants, L⁶⁴QQLL/A⁶⁴QQAA (termed AQQAA) and R90K, failed to alter NE morphology, subcellular Wee1-GFP distribution, or entry into mitosis (Web fig. 2). Thus Vpr, but not nonarresting mutants of Vpr, induced dynamic herniations in the NE that intermittently ruptured.

Vpr-induced changes in intracellular trafficking of Cdc25C and cyclin B1 were also examined. Both GFP-Cdc25C and cyclin B1-GFP principally localized in the cytoplasm during the S and G₂ phases (Fig. 2, A and I,

¹Gladstone Institute of Virology and Immunology, ²Department of Medicine and ³Department of Microbiology and Immunology, University of California, San Francisco, CA 94103, USA. ⁴Department of Cell and Molecular Biology, Northwestern University Medical School, Chicago, IL 60611, USA.

*To whom correspondence should be addressed. E-mail: wgreene@gladstone.ucsf.edu